

Analysis of Distance Protection for EHV Transmission Lines Using Artificial Neural Network

Ezema C.N¹, Iloh J.P.I², Obi P.I.³

^{1,2} Department of Electrical /Electronic Engineering, Chukwuemeka Odumegwu Ojukwu University, Anambra State, Nigeria

³ Department of Electrical/Electronic Engineering, Michael Okpara University of Agriculture, Umudike, Abia State, Nigeria.

Abstract— The main goal of this work is to locate fault in an electric power system with the optimal practically achievable accuracy. The method employed in this work makes use of phase voltages and phase currents (scaled with respect to their pre-fault values) as inputs to the neural networks. Typical faults such as single line-ground, line-line, double line-ground and three phase faults were considered and separate Artificial Neural Networks (ANNs) have been proposed for each of these faults. Since Back Propagation neural networks are very efficient when a sufficiently large training data set is available, it has been chosen for all the three steps in the fault location process namely fault detection, classification and fault location. The average and the maximum error percentages are in tolerable ranges and hence the network's performance is considered satisfactory. It can be seen that there is a steady decrease in the gradient and also that the number of validation fails did not exceed 1 during the entire process which indicates smooth and efficient training because the validation and the test phases reached the Mean Square Error performance (MSE) goal at the same time approximately.

Keywords— Double-Circuit Line Fault, Ground Fault Location, Line – Line Faults, Fault Location Algorithms.

I. INTRODUCTION

High voltage transmission lines cover long distances, hundreds of kilometers, particularly when the line passes through hilly and harsh terrains. When a fault occurs on these transmission lines it is extremely difficult to patrol the line from tower to tower to identify the faulty spot. Accurate identification and location of faults does not only save time but also saves power.

Power system operators need accurate information to enable speedy deployment of men and machinery to the fault's location in order to rectify the fault thereby saving lot of time and resources. Using software applications,

communication systems such as Supervisory Control and Data Acquisition (SCADA) and Power Line Carrier Communication (PLCC) hardware system can be designed for fault location. Data from SCADA such as oscillographs, relays and the sequence of events are used for fault location. Now available latest technology GPS can be used to locate a fault on long high voltage transmission lines. Self monitoring hardware devices are configured at foundation sites for both conditions by inserting the information of a fault location (GPS) into Geographical information system computer.

1.1 Existing Double-Circuit Line Fault Location Algorithms

Diverse fault location algorithms designed for double-circuit lines have been developed in the past few decades and will be henceforth reviewed. In the phasor-based fault location category, some methods utilize only one-terminal data to locate a fault. Akke & Thorp (2016) assume that the angles of a fault current and the fault current distribution from the load end are equal. They propose an algorithm that utilizes one-terminal voltage and current data. Because of their approximation the accuracy of their fault location is affected by the fault resistance and the asymmetrical arrangement of the transmission lines (Anderson, 2015).

Eriksson et al. (2016) employed phase voltages and currents from the near end of the faulted line, and a zero-sequence current from the near end of the healthy line as input signals. To fully compensate the error introduced by the fault resistance (or the impact of the remote in-feed), source impedance values are required.

Kawady and Stenzel (2014) used a modal transformation to decouple the initially coupled transmission lines. Their method utilizes as input voltage and current phasors from a locally installed relay. Compared with Eriksson et al. (2016), this algorithm does not need source impedances. It

modifies the apparent impedance seen from the relay location. This is, however, based on the assumption that the line is homogeneous. Simulations show that the accuracy is still sufficient when the algorithm is applied to an untransposed structure. Also, the effects of load current, shunt capacitance and fault resistance are negligible for the purpose of fault location.

Alessandro, Silvia & Ennio (1994) constructed a voltage equation from the local end through a faulty line to the fault point. Then they constructed another voltage equation from the local end, through a sound line and a faulty path, to the fault point. The remote in-feed can then be eliminated by inserting one equation into another. Then, three such equations for positive-, negative- and zero-sequence circuits were obtained. Next, based on the boundary conditions for different fault types, these three equations can be combined differently in order to solve for the fault resistance and the fault distance. Their algorithm is independent of fault resistance, load currents and source impedance. However, their model neglects shunt capacitance for long lines.

Non-earth faults on one of the circuits of parallel transmission lines are dealt with in (Das & Novosel, 2013). Similar to Dalstein & Kulicke (2016), the authors established three voltage equations from the local end via a faulty line to the fault point, based on three phase networks. Then these three equations are added, forming an equation with fault resistance and fault current as unknowns. Next, by applying the Kirchhoff voltage law (KVL) the fault current can be expressed as a function of fault distance. Solving for the fault resistance and the fault distance is then trivial. This algorithm is not influenced by fault resistance, load currents and source impedance. It, however, does not consider shunt capacitance, which will introduce errors for the fault location on long transmission lines.

The fault distance equations in (Cook, 2015) all include the current phasors of the adjacent sound line's local-end, which are assumed known. However, in some practical systems such current phasors are not available. Ahn et al. (2013) also construct the voltage equations that contain the sought-after fault resistance and fault location. By introducing the concept of current distribution factors the influence of the load current is eliminated. Since the formula for calculating the fault distance includes both local and remote source impedances, errors are introduced. The algorithm, however, is robust enough since it is largely insensitive to the variation in source impedances.

Izykowski et al. (2013) utilized all the voltage and current phasors of the local end from both the sound and the faulted lines as input. The zero-sequence impedance of a line will adversely influence the fault location accuracy. In the

expression for the fault path voltage drop, the weight of the zero-sequence fault current is set to zero to exclude the zero-sequence component. Since the fault distance formula does not contain any source impedances, the algorithm is neither influenced by the varying source impedances nor by the fault resistance.

Using a technique similar, Cichoki & Unbehauen (2013) have developed a fault location algorithm applicable to untransposed lines. It utilizes the lumped line model that ignores shunt capacitance. Because of that, the accuracy of the algorithm is not guaranteed for long transmission lines. In summary Bouthiba (2004) is similar in eliminating remote infeed. They achieved this by formulating appropriate Kirchhoff's Voltage Law (KVL) equations around the parallel lines loop.

Mazon et al. (2013) introduced a new concept of distance factor, which is the ratio of the positive-sequence pre-fault currents of both the sound and faulted lines at the local end. By comparing this value to the one calculated from system parameters when fault occurred, the fault location can be evaluated. Their algorithm is not affected by fault resistance or load current. Also, fault type classification is not necessary. However, the method is sensitive to variations in source impedances.

Next we will review two-terminal and multi-terminal algorithms. They usually provide more accurate fault location results than one-terminal algorithms, but require the synchronization of every terminal. Johns et al. (2015) provided a distributed-parameter based algorithm which fully considers the effect of shunt capacitance. It requires voltage and current phasors from both terminals of the faulted line. The algorithm is independent of fault resistance and source impedances. It does not require fault classification or synchronization of the two terminals. Although their method was designed for transposed lines, it also works satisfactorily when used for untransposed lines. Aurangzeb, Crossley & Gale (2011) have proposed an iterative approach to improve the accuracy of fault distance estimation in (Das & Novosel, 2013).

Lawrence et al. (2013) related the voltage and current phasors of the sending and receiving ends with ABCD parameters, where the fault distance and fault resistance are included. For different types of fault, different equations are derived. The synchronized phasors of two terminals are needed to feed the algorithm. The method can also be used for untransposed lines, and is independent of fault resistance and source impedances.

Nagasawa et al. (2013) present an algorithm based on the lumped parameter model, which may introduce errors for long lines. The procedure needs only the magnitude of the

differential current of each terminal. It is the difference of the currents in both circuits measured at the same terminal. Since their method was developed for three-terminal parallel transmission lines, any n-terminal network must be converted to an equivalent three-terminal network first. Because only the magnitudes of differential currents are required, synchronization of the terminals is not necessary. The algorithm is independent of fault resistance and of any source impedances. Furthermore, it does not demand fault classification. However, the approach is designed for transposed transmission lines only.

Funabashi et al. (2011) have presented multi-terminal algorithms based on the lumped parameter model. Their algorithm 1 is based on an impedance calculation that makes use of phase current data at each terminal, phase voltage data at the locator terminal, and all the phase components of the line impedance. Algorithm 2 introduces the current diversion ratio method. It utilizes phase current data at each terminal and all the phase components of the line impedance. Both algorithms are applicable to all types of single-circuit or inter-circuit faults. The fault location is independent of fault resistance and the method does not require knowledge of source impedances. Since the phase component of the line impedance is utilized it is suitable both for balanced and unbalanced lines. Fault classification is irrelevant for this algorithm, but synchronization of the terminal voltages and currents is needed.

In the realm of time-domain fault location methods, Bo, Weller & Redfern (2009) decomposes the transmission lines into a common component net and a differential component net, each of which is a single-circuit network. For the differential component net the voltages at both terminals are zero. Based on the distributed parameter time-domain equivalent model, two voltage distributions along the line can be calculated from the two terminal currents, respectively. The proposed approach exploits the fact that the difference between these two voltages is smallest at the point of fault. The algorithm has the following advantages:

- A data window less than one cycle long, satisfying high-speed tripping requirements.
- No requirement to synchronize the two terminal currents.
- No need for voltage data.
- No source impedance exists in the differential component net.

- Independence from fault resistance.
- Full account of the influence of shunt capacitance.
- Suitable both for the transposed and untransposed lines.

All the existent algorithms for double-circuit transmission lines have different advantages. Unfortunately, these methods share a common drawback, namely that the measurements have to be taken from one or two terminals of the faulted section, or even at all the terminals of the entire network. From a practical point of view the data may not be available at the terminals of the faulted line, let alone from all the buses. Hence, this research work will bridge the gap by analyzing distance protection for EHV transmission lines using artificial neural network modules.

II. MATERIALS AND METHOD

The method employed in this work makes use of phase voltages and phase currents (scaled with respect to their pre-fault values) as inputs to the neural networks. Possible kinds of faults such as single line-ground, line-line, double line-ground and three phase faults were considered and separate ANNs have been proposed for each of these faults. Since Back Propagation neural networks are very efficient when a sufficiently large training data set is available, it has been chosen for all the three steps in the fault location process namely fault detection, fault classification and fault location.

The main goal of fault diagnosis is to locate fault in an electric power system with the highest practically achievable accuracy. When the physical dimensions and size of the transmission lines are considered, the accuracy with which the designed fault locator locates faults in the power system becomes very important.

The fundamental principle of the proposed fault location method is to add to the original network a fictitious bus where the fault occurs as shown in Figure 1. Hence, the bus impedance matrix is augmented by one order. Then, the driving point impedance of the fault bus and the transfer impedances between this bus and other buses are expressed as functions of the unknown fault distance. Based on the definition of the bus impedance matrix, the change of the sequence voltage at any bus during the fault is formulated in terms of the corresponding transfer impedance and sequence fault current. Depending on the boundary conditions for different fault types, we can obtain the fault location equation using voltage phasors as input.

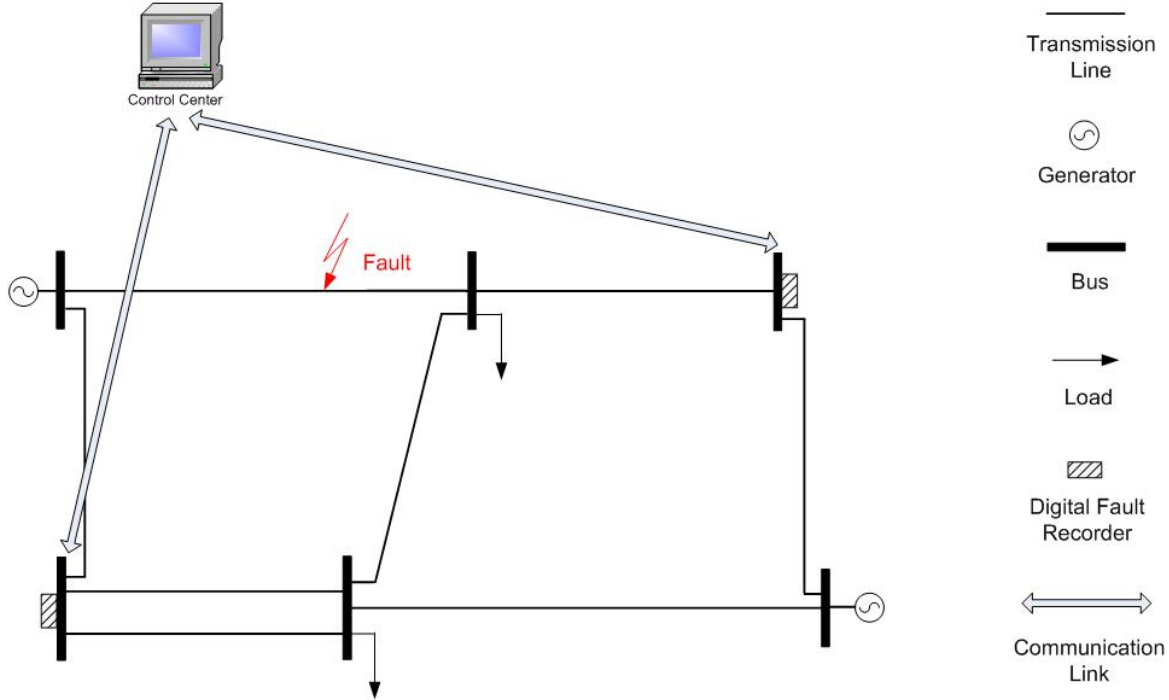


Fig.1: A sample wide area monitoring system.

Based on the same augmented bus impedance matrix, Voltage and Current Relation (VCR) are employed. Now the change of the current at any branch can be expressed as a function of the relevant fault current and the transfer impedance terms associated with the two ends of the branch. Fault location model takes fully into account the shunt capacitance. With different boundary conditions for the various fault types, the unknown fault location can be obtained by properly formulating the fault currents and voltages at the fault point. Two subroutines assuming that the fault occurs on either side of the series compensator are developed. A prescription to distinguish the correct fault location from the erroneous one is provided.

Therefore, this paper presents a system that is capable of detecting and locating the fault with less proportion of error. This system uses the global positioning system (GPS) to locate the position and the global system for mobile (GSM) to send these messages to system supervisor.

III. RESULTS AND DISCUSSION

3.1 Testing the Neural Network for Single Line – Ground Fault Location

Several factors have been considered while testing the performance of the neural networks. One prime factor that evaluates the efficiency of the ANN is the test phase performance. As already mentioned, the average and the maximum error percentages are in tolerable ranges and hence the networks performance is considered satisfactory. Another form of analysis is provided by Figure 3, which is the gradient and validation performance plot. It can be seen that there is a steady decrease in the gradient and also that the number of validation fails are 0 during the entire process which indicates smooth and efficient training.

The third factor considered while evaluating the performance of the network is the correlation coefficient of each of the various phases of training, validation and testing. Figure 2 shows the regression plots of the various phases such as training, testing and validation. It can be seen that the best linear fit very closely matches the ideal case with an overall correlation coefficient of 0.99924.

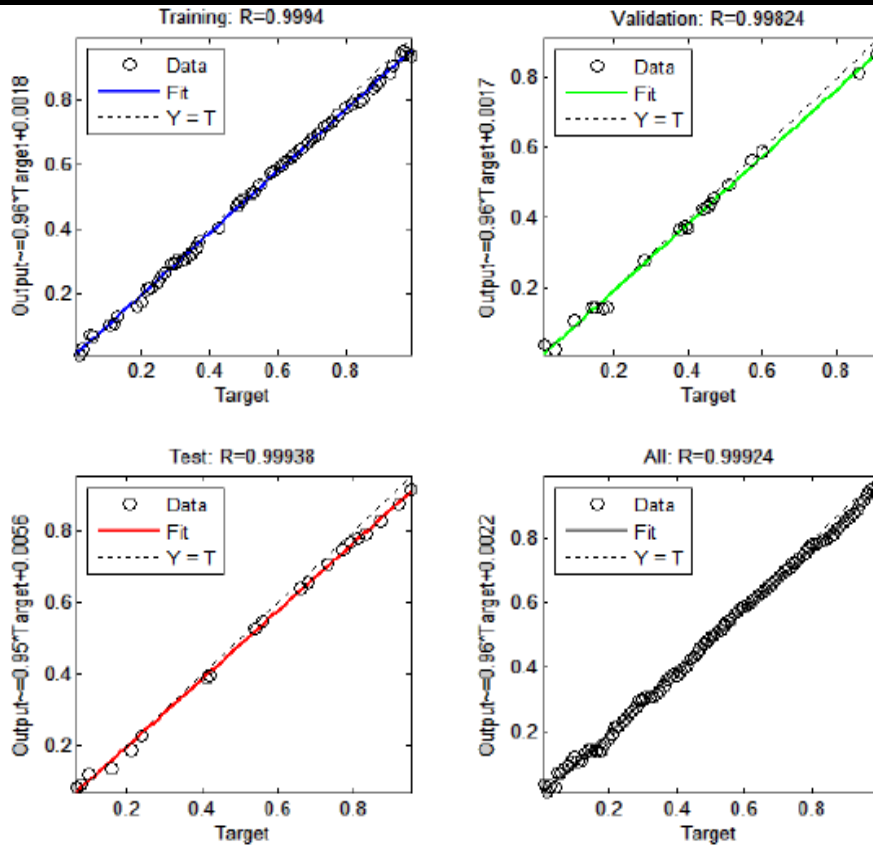


Fig.2: Regression plots of various phases of learning of the ANN with configuration (6-7-1).

Figure 3 shows the structure of the chosen ANN for single line – ground faults with 6 neurons in the input layer, 7 neurons in the hidden layer and 1 neuron in the output layer (6-7-1).

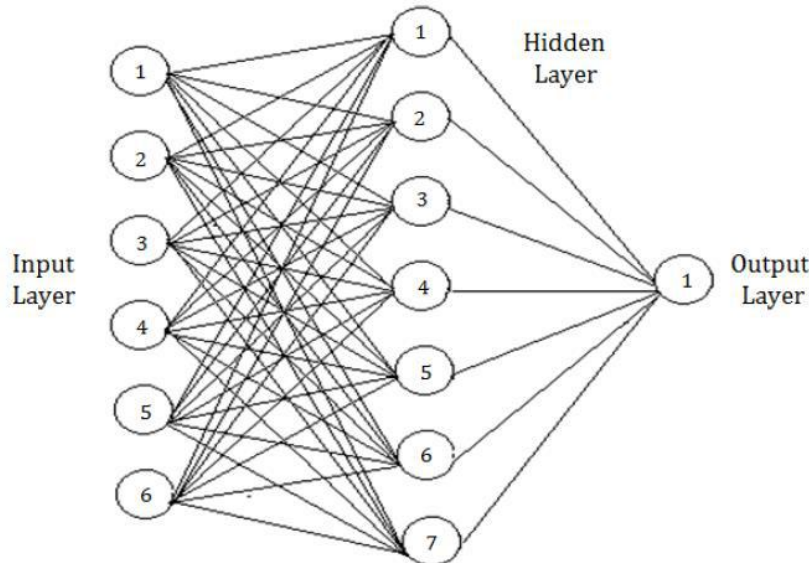


Fig.3: Structure of the chosen ANN with configuration (6-7-1).

Table 1 illustrates the percentage errors in Fault location as a function of Fault Distance and Fault Resistance. Two different cases have been considered (shown in adjacent

columns), one with a fault resistance of 20 ohms and another with a fault resistance of 60 ohms. It is to be noted that the resistance of 20 ohms was used as a part of training

data set and hence the average percentage error in fault location in this case is just 0.1646 %. The second case illustrates the same with a different fault resistance of 60 ohms which is relatively very high and is not a part of the training set. Hence, the performance of the neural network

in this case illustrates its ability to generalize and react upon new data. It is to be noted that the average error in this case is just 0.878 % which is very satisfactory. Thus the neural networks performance is considered satisfactory and can be used for the purpose of single line – ground fault location.

Table.1: Percentage errors as a function of fault distance and fault resistance for the ANN chosen for single line - ground fault location.

| Serial No: | % Error vs. Fault Distance (Fault Resistance = 20 Ω) | | | % Error vs. Fault Distance (Fault Resistance = 60 Ω) | | |
|------------|---|-------------------------|------------------|---|-------------------------|------------------|
| | Fault Resistance (Ω) | Measured Fault Location | Percentage Error | Fault Distance (Km) | Measured Fault Location | Percentage Error |
| 1 | 25 | 25.49 | 0.163 | 50 | 51.56 | 0.52 |
| 2 | 75 | 75.58 | 0.287 | 100 | 101.02 | 0.34 |
| 3 | 125 | 125.12 | 0.04 | 150 | 153.03 | 1.01 |
| 4 | 175 | 175.09 | 0.03 | 200 | 202.67 | 0.89 |
| 5 | 225 | 225.91 | 0.303 | 250 | 254.89 | 1.63 |

3.2 Line – Line Faults

The design, development and performance of neural networks for the purpose of Line – Line fault location are discussed in this section. Now that we can detect the occurrence of a fault on a transmission line and also classify the fault into the various fault categories, the next step is to pin-point the location of the fault from either ends of the transmission line. Three possible line – line faults exist (A-B, B-C, C-A), corresponding to each of the three phases (A, B or C) being faulted.

3.2.1 Training the Neural Network for Line – Line Fault Location

Feed forward back – propagation neural networks have been surveyed for the purpose of line – line fault location, mainly because of the availability of sufficient data to train the network. In order to train the neural network, several line – line faults have been simulated on the transmission line model. For each pair formed by the three phases, faults have been simulated at every 3 Km along a 300 Km long transmission line. Along with the fault distance, the fault resistance has been varied as 0.25, 0.5, 0.75, 1, 5, 10, 25 and 50 ohms respectively. Hence, a total of 2400 cases have been simulated (100 for each of the three phases with each of the eight different fault resistances). In each of these cases, the voltage and current samples for all three phases

(scaled with respect to their pre-fault values) are given as inputs to the neural network. The output of the neural network is the distance to the fault from terminal A. Hence, each input output pair consists of six inputs and one output. An exhaustive survey on various neural networks has been performed by varying the number of hidden layers and the number of neurons per hidden layer. Certain neural networks that achieved satisfactory performance are presented first along with their error performance plots. Of these ANNs, the most appropriate ANN is chosen based on its Mean Square Error (MSE) performance and the Regression coefficient of the Outputs versus Targets. Figures 4 – 5 show the MSE and the Test phase performance plots of the neural networks 6 – 10 – 20 – 5 – 1 with 3 hidden layers. Figures 6 – 7 show the MSE and the Test phase performance plots of the neural network 6 – 10 – 1 with 1 hidden layer.

Figure 4 shows the performance of the neural network (in terms of training, testing and validation) with 6 neurons in the input layer, 3 hidden layers with 10, 20 and 5 neurons in them respectively and 1 neuron in the output layer (6 – 10 – 20 – 5 – 1). It can be seen that the best MSE performance of this neural network is 0.0073438 which is below the MSE goal of 0.01. It was found that the correlation coefficient between the outputs and the targets was 0.98469 in this case.

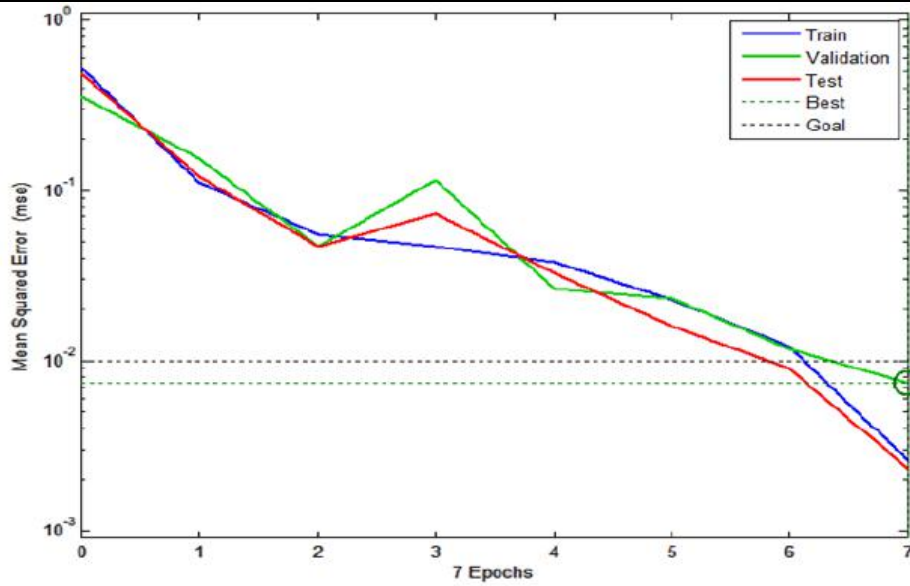


Fig.4: Mean Square Error performance plot with configuration (6-10-20-5-1).

In order to test the performance of this network, 12 different line – line faults have been simulated on different phases with the fault distance being incremented by 25 km in each case and the percentage error in calculated output has been

calculated. Figure 5 shows the results of this test conducted on the neural network (6-10-20-5-1). It can be seen that the maximum error is around 2.75 percent.

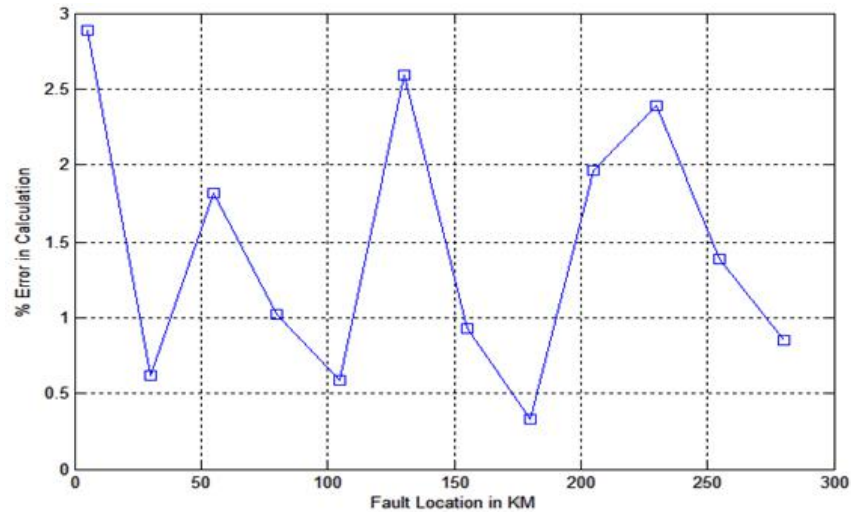


Fig.5: Test Phase performance of the ANN with configuration (6-10-20-5-1).

Figure 6 shows the performance of the neural network (in terms of training, testing and validation) with 6 neurons in the input layer, 10 neurons in the hidden layer and 1 neuron in the output layer (6 – 10 – 1). It can be seen that the best

MSE performance of this neural network is 0.0045535 which is below the MSE goal of 0.01. It was found that the correlation coefficient between the outputs and the targets was 0.9825 for this neural network.

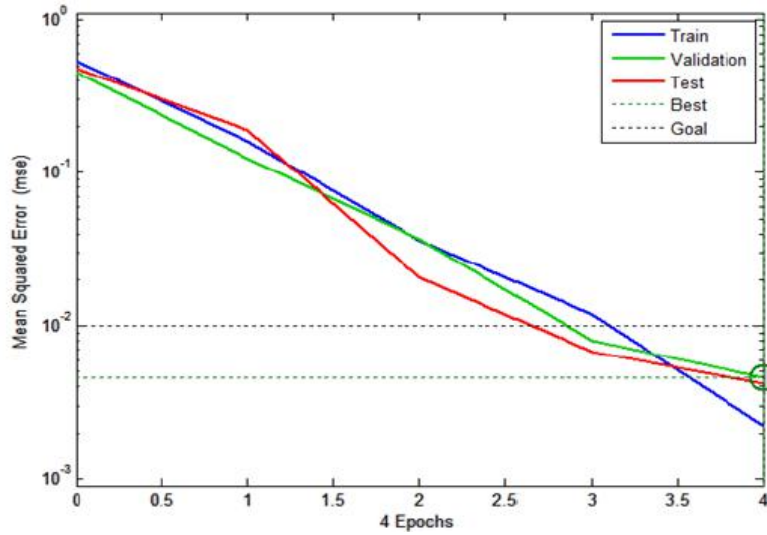


Fig.6: Mean Square Error performance plot with configuration (6-10-1).

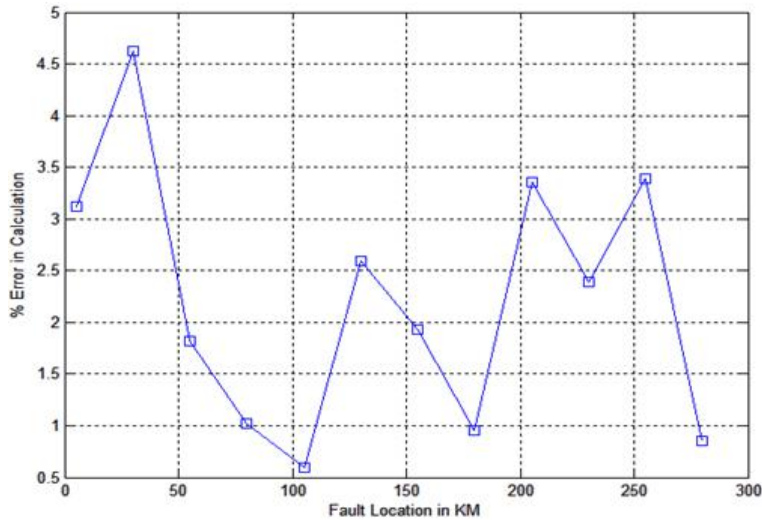


Fig.7: Test Phase performance of the ANN with configuration (6-10-1).

In order to test the performance of this network, 12 different line – line faults have been simulated on different phases with the fault distance being incremented by 25 Km in each case and the percentage error in calculated output has been calculated. Figure 7 shows the results of this test conducted on the neural network (6-10-1). It can be seen that the maximum error is around 4.65 percent which is unacceptable.

Figure 8 shows the performance of the neural network (in terms of training, testing and validation) with 6 neurons in the input layer, 2 hidden layers with 10 and 5 neurons in them respectively and 1 neuron in the output layer (6 – 10 – 5 – 1). It can be seen that the best MSE performance of this neural network is 0.002089 which is below the MSE goal of 0.01. It was found that the correlation coefficient between the outputs and the targets was 0.98648 for this neural network.

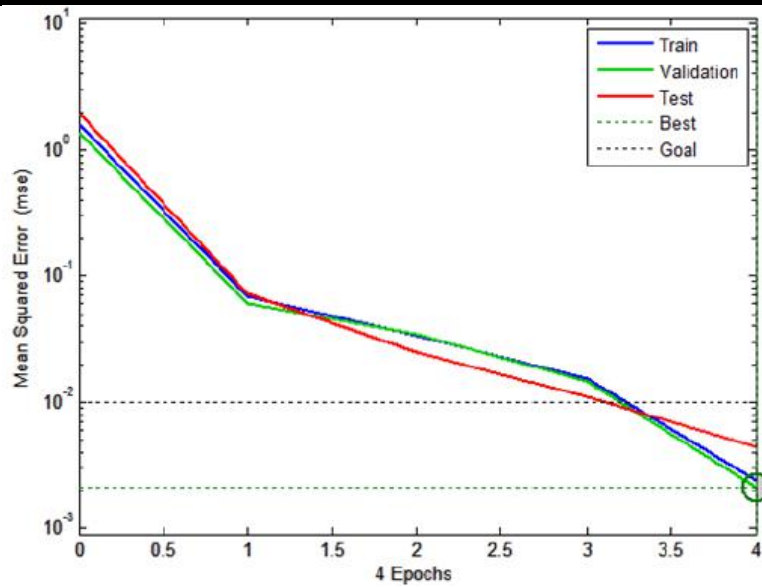


Fig.8: Mean Square Error performance of the ANN with configuration (6-10-5-1)

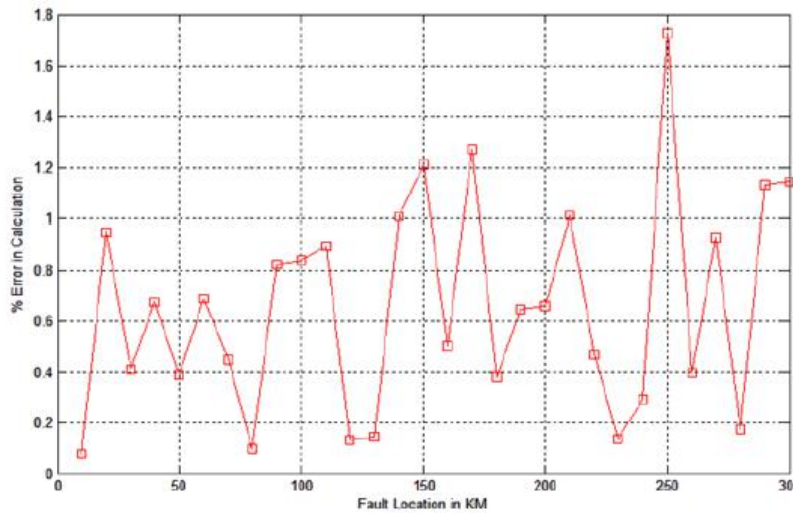


Fig.9: Test phase performance of the neural network with configuration (6-10-5-1).

In order to test the performance of this network, 100 different phase to phase faults have been simulated on different phases with the fault distance being incremented by 10 Km in each case and the percentage error in calculated output has been calculated.

Figure 9 shows the results of this test conducted on the neural network (6-10-5-1). It can be seen that the maximum error is around 1.7 percent which is very satisfactory. It is to be noted that the average error in fault location is just 0.97 percent. Hence, this neural network has been chosen as the

ideal network for the purpose of line – line fault location on transmission lines.

Figure 10 shows an overview of the chosen ANN and it can be seen that the training algorithm used is Levenberg - Marquardt algorithm. The performance function chosen for the training process is mean square error. Figure 11 plots the plots the best linear regression fit between the outputs and the targets and the correlation coefficient for the same has been found to be 0.98648 which is a decently good regression fit.

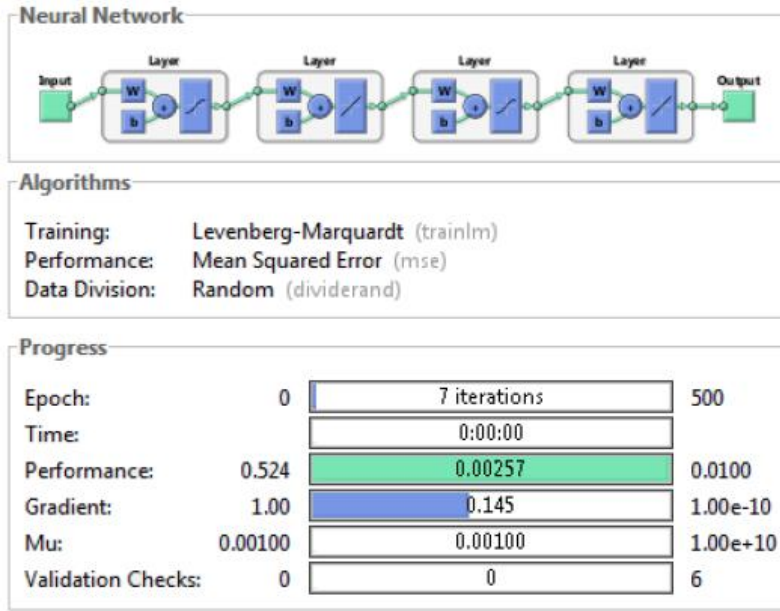


Fig.10: Overview of the chosen ANN for Line-Line Faults (6-10-5-1).

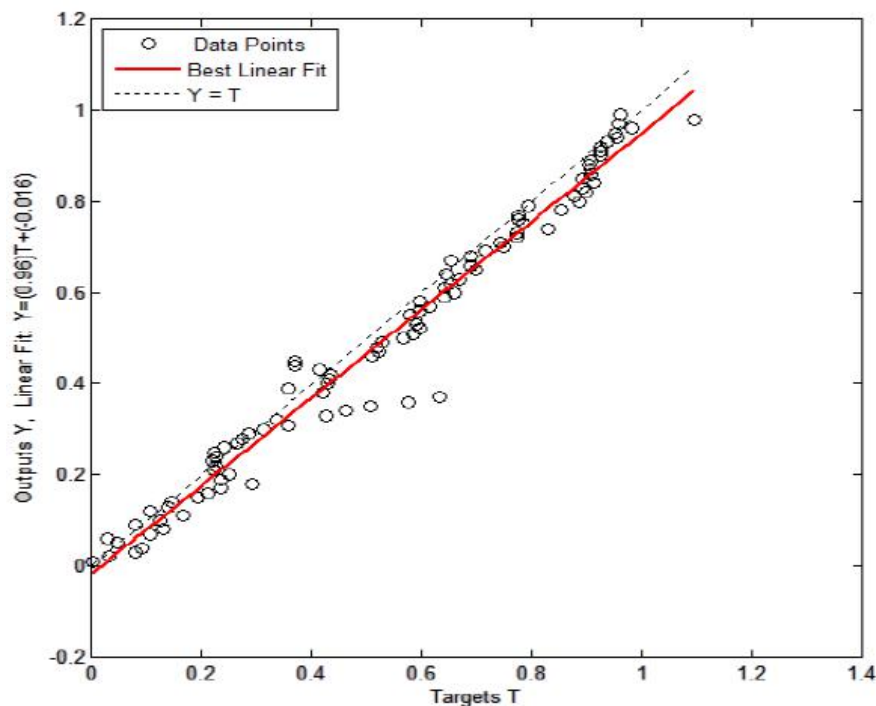


Fig.11: Regression fit of the outputs versus targets with configuration (6-10-5-1).

3.2.2 Testing the Neural Network For Line – Line Fault Location

Several factors have been considered while testing the performance of the chosen neural network. One prime factor that evaluates the efficiency of the ANN is the test phase performance plot which is already illustrated in Figure 11. As already mentioned, the average and the maximum error percentages are in tolerable ranges and

hence the network’s performance is considered satisfactory. Another means of evaluating the ANN is provided by Figure 12, which is the gradient and validation performance plot.

It can be seen that there is a steady decrease in the gradient and also that the number of validation fails did not exceed 1 during the entire process which indicates smooth and

efficient training because the validation and the test phases reached the MSE goal at the same time approximately.

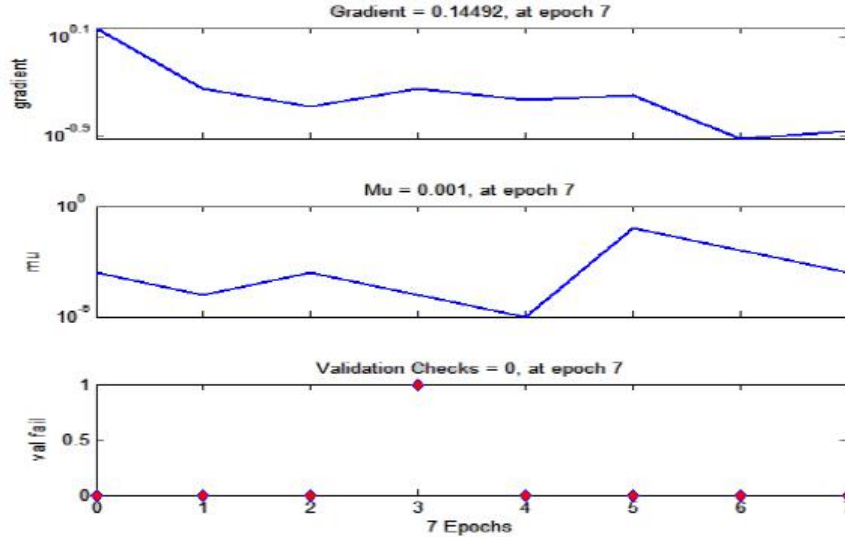


Fig.12: Gradient and validation performance plot of the ANN (6-10-5-1).

The third factor that is considered while evaluating the performance of the network is the correlation coefficient of each of the various phases of training, validation and testing. Figure 13 shows the regression plots of the various

phases such as training, testing and validation. It can be seen that the best linear fit very closely matches the ideal case with an overall correlation coefficient of 0.98648.

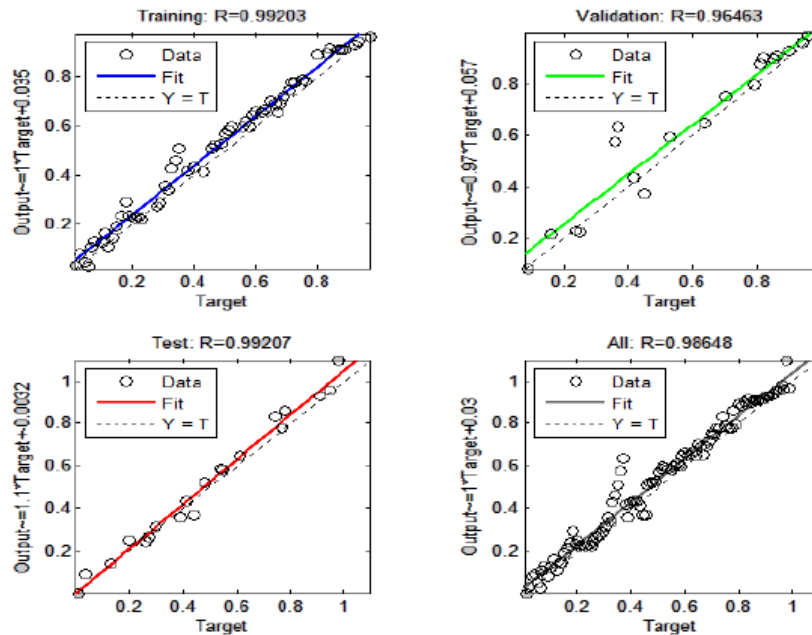


Fig.13: Regression plots of the various phases of learning of the chosen ANN (6-10-5-1).

Figure 14 shows the structure of the chosen ANN for line – line faults with 6 neurons in the input layer, 2 hidden layers

with 10 and 5 neurons in them respectively and 1 neuron in the output layer (6 – 10 – 5 – 1).

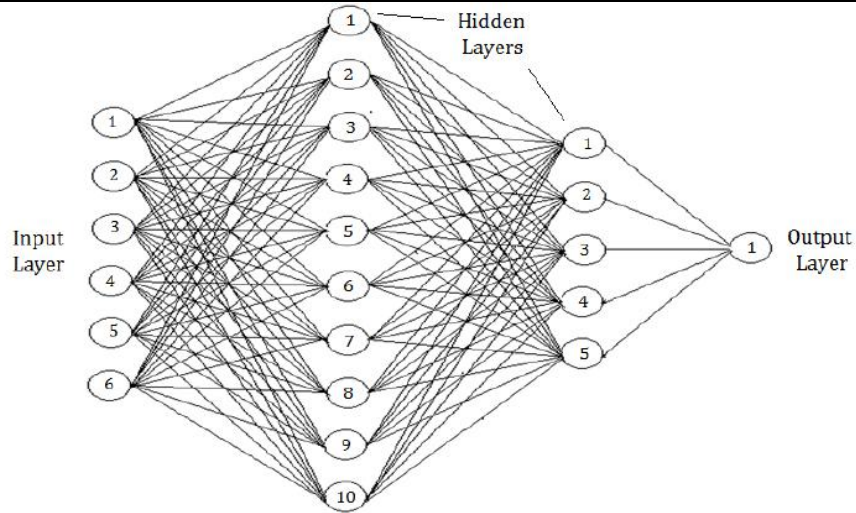


Fig.14: Structure of the chosen Neural Network (6 – 10 – 5 – 1).

Table 2 illustrates the percentage errors in Fault location as a function of Fault Distance and Fault Resistance. Two different cases have been considered (shown in adjacent columns), one with a fault resistance of 20 ohms and another with a fault resistance of 60 ohms. It is to be noted that the resistance of 20 ohms was used as a part of training data set and hence the average percentage error in fault location in this case is just 0.1386 %. The second case

illustrates the same with a different fault resistance of 60 ohms which is relatively very high and is not a part of the training set. Hence, the performance of the neural network in this case illustrates its ability to generalize and react upon new data. It is to be noted that the average error in this case is just 0.966 % which is still very satisfactory. Thus the neural networks performance is considered satisfactory and can be used for the purpose of line – line fault location.

Table.2 Percentage errors as a function of fault distance and fault resistance for the ANN chosen for line - line fault location.

| Serial No: | % Error vs. Fault Distance (Fault Resistance = 20 Ω) | | | % Error vs. Fault Distance (Fault Resistance = 60 Ω) | | |
|------------|---|-------------------------|------------------|---|-------------------------|------------------|
| | Fault Distance (Km) | Measured Fault Location | Percentage Error | Fault Distance (Km) | Measured Fault Location | Percentage Error |
| 1 | 25 | 25.03 | 0.01 | 50 | 51.17 | 0.39 |
| 2 | 75 | 75.39 | 0.13 | 100 | 102.52 | 0.84 |
| 3 | 125 | 125.67 | 0.223 | 150 | 153.63 | 1.21 |
| 4 | 175 | 175.14 | 0.047 | 200 | 201.98 | 0.66 |
| 5 | 225 | 225.85 | 0.283 | 250 | 255.19 | 1.73 |

Table 3 illustrates the percentage errors in Fault location as a function of Fault Distance and Fault Resistance. Two different cases have been considered (shown in adjacent columns), one with a fault resistance of 20 ohms and another with a fault resistance of 60 ohms. It is to be noted that the resistance of 20 ohms was used as a part of training data set and hence the average percentage error in fault location in this case is just 0.091 %. The second case

illustrates the same with a different fault resistance of 60 ohms which is relatively very high and is not a part of the training set. Hence, the performance of the neural network in this case illustrates its ability to generalize and react upon new data. It is to be noted that the average error in this case is just 1.122 % which is still acceptable. Thus the neural networks performance is considered satisfactory and can be used for the purpose of double line – ground fault location.

Table.3: Percentage errors as a function of fault distance and fault resistance for the ANN chosen for double line - ground fault location.

| Serial No: | % Error vs. Fault Distance (Fault Resistance = 20 Ω) | | | % Error vs. Fault Distance (Fault Resistance = 60 Ω) | | |
|------------|---|-------------------------|------------------|---|-------------------------|------------------|
| | Fault Distance (Km) | Measured Fault Location | Percentage Error | Fault Distance (Km) | Measured Fault Location | Percentage Error |
| 1 | 25 | 25.53 | 0.177 | 50 | 53.81 | 1.27 |
| 2 | 75 | 75.18 | 0.06 | 100 | 103.12 | 1.04 |
| 3 | 125 | 125.11 | 0.037 | 150 | 152.13 | 0.71 |
| 4 | 175 | 175.16 | 0.053 | 200 | 202.88 | 0.96 |
| 5 | 225 | 225.39 | 0.13 | 250 | 254.89 | 1.63 |

Table 4 illustrates the percentage errors in Fault location as a function of Fault Distance and Fault Resistance. Two different cases have been considered (shown in adjacent columns), one with a fault resistance of 20 ohms and another with a fault resistance of 60 ohms. It is to be noted that the resistance of 20 ohms was used as a part of training data set and hence the average percentage error in fault location in this case is just 0.178 %. The second case

illustrates the same with a different fault resistance of 60 ohms which is relatively very high and is not a part of the training set. Hence, the performance of the neural network in this case illustrates its ability to generalize and react upon new data. It is to be noted that the average error in this case is just 0.836 % which is still acceptable. Thus the neural networks performance is considered satisfactory and can be used for the purpose of three phase fault location.

Table.4: Percentage errors as a function of fault distance and fault resistance for the ANN chosen for three phase fault location.

| Serial No: | % Error vs. Fault Distance (Fault Resistance = 20 Ω) | | | % Error vs. Fault Distance (Fault Resistance = 60 Ω) | | |
|------------|---|-------------------------|------------------|---|-------------------------|------------------|
| | Fault Distance (Km) | Measured Fault Location | Percentage Error | Fault Distance (Km) | Measured Fault Location | Percentage Error |
| 1 | 25 | 25.51 | 0.17 | 50 | 51.41 | 0.47 |
| 2 | 75 | 75.17 | 0.057 | 100 | 103.03 | 1.01 |
| 3 | 125 | 125.52 | 0.28 | 150 | 152.37 | 0.79 |
| 4 | 175 | 175.69 | 0.23 | 200 | 201.99 | 0.63 |
| 5 | 225 | 225.46 | 0.1533 | 250 | 253.84 | 1.28 |

IV. CONCLUSION

It is very essential to investigate and analyze the advantages of a particular neural network structure and learning algorithm before choosing it for an application because there should be a trade-off between the training characteristics and the performance factors of any neural network.

This research work has shown that the lower the sampling frequency, the lesser the computational burden on the industrial PC that uses the neural networks. This means a lot of energy savings because a continuous online detection scheme of this kind consumes a large amount of energy, a major portion of which is due to the continuous sampling of waveforms. The above mentioned are some significant

improvements that this work offers over existing neural network based techniques for transmission line fault diagnosis.

REFERENCES

- [1] Anderson, P. M. (1995). *Analysis of Faulted Power Systems*, IEEE Press Power System Engineering Series, Wiley-IEEE Press, New York.
- [2] Akke, M., & Thorp, J. T. (2016). *Some Improvements in the Three-Phase Differential Equation Algorithm for Fast Transmission Line Protection*. IEEE Transactions on Power Delivery, vol. 13, pp. 66-72.
- [3] Alessandro, F., Silvia, S., & Ennio, Z. A (1994). *Fuzzy-Set Approach to Fault-Type Identification in Digital Relaying, Transmission and Distribution*. Conference, Proceedings of the IEEE Power Engineering Society, vol. 64 pp. 269-275.
- [4] Aurangzeb, M., Crossley, P. A., & Gale, P. (2011). *Fault Location Using High Frequency Travelling Waves Measured at a Single Location on Transmission Line*. Proceedings of 7th International conference on Developments in Power System Protection – DPSP, IEE, vol. CP479, pp. 403-406.
- [5] Bo, Z. Q., Weller, G., & Redfern, M. A. (2009). *Accurate Fault Location Technique For Distribution System Using Fault-Generated High Frequency Transient Voltage Signals*. IEEE Proceedings of Generation, Transmission and Distribution, vol. 146(1), pp. 73-79.
- [6] Bouthiba T. (2004). *Fault location in EHV Transmission Lines Using Artificial Neural Networks*. International Journal of Applied Mathematics & Computational Science, vol. 14(1), pp. 69-78.
- [7] Cichoki, A., & Unbehauen, R. (2013). *Neural Networks for Optimization and Signal Processing*. John Wiley & Sons, Inc. New York.
- [8] Cook, V. (2015). *Analysis of Distance Protection*. Research Studies Press Ltd., John Wiley & Sons, Inc., New York.
- [9] Cook, V. (2012). *Fundamental Aspects of Fault Location Algorithms Used in Distance Protection*. Proceedings of IEE Conference, vol. 133(6), pp. 359-368.
- [10] Dalstein, T., & Kulicke, B. (2016). *Neural Network Approach to Fault Classification for High Speed Protective Relaying*. IEEE Transactions on Power Delivery, vol. 4, pp. 1002 – 1009.
- [11] Das, R., & Novosel, D. (2013). *Review of Fault Location Techniques For Transmission and Sub – Transmission Lines*. Proceedings of 54th Annual Georgia Tech Protective Relaying Conference, vol. 4, pp. 61-83
- [12] Eriksson, L. & Rockefeller, G., D. (2015). *An Accurate Fault Locator with Compensation for Apparent Reactance in the Fault Resistance Resulting from Remote-End Feed*. IEEE Trans on PAS, vol. 104(2), pp. 424-436.
- [13] Girgis, A. A., Hart, D. G., & Peterson, W. L. (1992). *A New Fault Location Techniques for Two and Three Terminal Lines*. IEEE Transactions on Power Delivery vol. 7(1), pp. 98-107.
- [14] Haykin, S. (1994). *Neural Networks: A Comprehensive Foundation*. Macmillan Collage Publishing Company, Inc. New York.
- [15] Howard, D., Mark, B., & Martin, H. (2012). *The MathWorks User's Guide for MATLAB and Simulink*. Neural Networks Toolbox 6.
- [16] IEEE Guide for Determining Fault Location on AC Transmission and Distribution Lines. (2015). IEEE Power Engineering Society Publication. New York, IEEE Std, vol. C37. pp. 114.
- [17] Karl Z., & David C. (2015). *Impedance-Based Fault Location Experience*. Schweitzer Engineering Laboratories, Inc. Pullman, WA USA.
- [18] Kasztenny, B., Sharples, D., & Asaro, V. (2011). *Distance Relays and capacitive voltage transformers – balancing speed and transient overreach*. Proceedings of 55th Annual Georgia Tech Protective Relaying Conference, vol. 2, pp. 6-15.
- [19] Lahiri, U., Pradhan, A. K., & Mukhopadhyaya, S. (2015). *Modular Neural-Network Based Directional Relay for Transmission Line Protection*. IEEE Trans. on Power Delivery, vol. 20(4), pp. 2154-2155.
- [20] Magnago, H., & Abur, A. (2009). *Advanced Techniques for Transmission and Distribution System Fault Location*. Proceedings of CIGRE – Study Committee 34 Colloquium and Meeting, Florence, vol. 8, pp. 215.
- [21] Network Protection & Automation Guide. (2016). *T&D Energy Automation & Information*. Alstom, France.